# Vacancy model for substitutional $Ni^-$, $Pd^-$, $Pt^-$, and $Au^0$ in silicon

G. D. Watkins and P. M. Williams
*Department of Physics, Lehigh University, 16 Memorial Drive East, Bethlehem, Pennsylvania 18015*
(Received 14 April 1995; revised manuscript received 2 August 1995)

The vacancy model for the electronic structure in silicon of substitutional transition elements near the end of the 3*d*, 4*d*, and 5*d* series is described and a simplified theoretical treatment for their paramagnetic properties is presented. It is concluded that the complete set of such impurities for which experimental information is available—$Ni_s^-$, $Pd_s^-$, $Pt_s^-$, and $Au_s^0$—are all well described by the model. In making this argument, an alternative, physically more reasonable, analysis is proposed for the electron paramagnetic resonance and electron-nuclear double resonance results on $Ni_s^-$ and $Pd_s^-$ [Solid State Commun. **80**, 439 (1991)], which were originally interpreted as conflicting with the model.

## I. INTRODUCTION

Several years ago, one of us suggested a model for the electronic structure in silicon of substitutional transition element impurities near the end of the $3d^n$, $4d^n$, and $5d^n$ series.[1] Labeled the "vacancy model," it described the structure as primarily that of a filled *d* shell deep in the valence band, with the remaining electrons in the $t_2$ vacancylike orbitals of the four silicon neighbors, which are in the forbidden gap and account for the electrical activity of the defect. The rationale was the recognition that for these impurities, the *d*-shell orbitals are energetically much lower than those of the dangling vacancy orbitals with which they overlap, and they should therefore be filled first. In this model, only small admixtures of the $d(t_2)$ orbitals should be present in the vacancy $t_2$ orbitals. The evidence cited at the time was early electronic structure calculations that demonstrated such a trend.[2] Subsequent more sophisticated electronic structure calculations have also been interpreted to confirm the model.[3–6]

Experimentally, however, the model has proven to be one of continuing controversy. Initially, the controversy centered on the interpretation of electron paramagnetic resonance (EPR) studies of substitutional $Pt^-$ ($Pt_s^-$), where an alternative dihedral bonding model with the unpaired electron in the 5*d* shell was put forward.[7] The argument of these authors was based primarily on the observed *g* values, which were argued to be incompatible with the vacancy model. Subsequently, however, Delerue, Lanoo, and Allan[8] and Anderson *et al.*,[9] using a phenomenological approach introduced by Lowther[10] for the problem, showed that the *g* values and central ion hyperfine values could be fitted well within the vacancy model. Finally, Anderson, Ham, and Watkins[11] showed from a detailed theoretical treatment that all of the general features of the EPR spectrum—the *g* values, the hyperfine interactions with the Pt and only two of its silicon neighbors, and the behavior under uniaxial stress—could be adequately accounted for in the vacancy model.

More recently, the controversy has shifted to the 4*d* and 3*d* counterparts, $Pd_s^-$ and $Ni_s^-$. In these cases, an analysis of the hyperfine interactions for the transition element impurity, as observed by EPR and electron-nuclear double resonance (ENDOR), was interpreted to indicate the *symmetry* of the orbital containing the paramagnetic electron to be inconsistent with the vacancy model.[12,13] In the present paper, however, we will point out an alternative analysis of the experimental results, which we argue is physically more reasonable, and which can also match the experimental data. This analysis provides hyperfine interactions which are now consistent with the vacancy model, as are the other properties of these centers. In addition, we will show that the vacancy model provides a unique and natural explanation for the unusual properties of substitutional $Au_s^0$. We conclude, therefore, that the vacancy model successfully accounts for the properties of all the substitutional transition element impurities near the end of the $3d^n$, $4d^n$, and $5d^n$ series which have so far been determined in silicon.

The outline of the paper is as follows: In Sec. II, we present a brief summary of the vacancy model. We present a simplified treatment of the theory of Anderson, Ham, and Watkins[11] for the spin-Hamiltonian parameters, which retains the essential physics of the problem, identifying it as a competition between spin-orbit interaction and a Jahn-Teller off-center $C_{2v}$ distortion of the impurity ion, and we summarize the agreement achieved for the $Pt_s^-$ EPR results. In Sec. III, we show, using this simple treatment, that the vacancy model explains also in a natural way the properties of substitutional $Au_s^0$, as deduced via recent Zeeman studies of its optical hole and electron excitation spectra.[19,20] In Sec. IV, we review the experimental EPR results for $Pd_s^-$ and $Ni_s^-$, and demonstrate that their *g* values and Jahn-Teller distortion characteristics are also well explained by the vacancy model. We then consider the hyperfine analysis and conclusions as presented in Refs. 12 and 13. We point out an alternative analysis to their results, which we argue is physically more realistic, and demonstrate that it now leads to satisfactory agreement with the vacancy model. In Sec. V we summarize.

0163-1829/95/52(23)/16575(6)/$06.00  

## II. THE VACANCY MODEL

The basic idea of the vacancy model is illustrated in Fig. 1. The vacancy $t_2$ states that lie in the band gap result from the dangling bonds on the silicon atoms surrounding the vacant site into which the transition element ($X$) is inserted. They interact weakly with the impurity $d$ states of $t_2$ symmetry, which are filled, being deep in the valence band for transition-element ions at the end of each series, and remain strongly vacancylike, containing therefore only small admixtures of the impurity $d$ states. For $Ni_s^-$, $Pd_s^-$, $Pt_s^-$, and $Au_s^0$ there are three electrons in the $t_2$ orbital, similar to the case for the isolated vacancy ($V^-$).

As for $V^-$, the degeneracy can be lifted by a tetragonal Jahn-Teller (JT) distortion, plus a weaker trigonal one, to give $C_{2v}$ symmetry,[14] as illustrated in Figs. 2(a)–2(c). This observation of $C_{2v}$ symmetry for both $Pt_s^-$ and $V^-$ was cited as a supporting argument in the original proposal of the vacancy model.[1] Subsequent studies of alignment under uniaxial stress[15] revealed that for $Pt_s^-$, the sign of each distortion is actually reversed from that for $V^-$, giving the signs illustrated in Fig. 2(e)—heavy arrows for the tetragonal distortion and light arrows for the $t_{2z}$ trigonal distortion—and the ordering of the levels shown in the figure. (Linear JT coupling predicts for the three-electron case equal energy gains for either sign of distortion,[11,16] the actual choice being determined by higher-order effects. The difference presumably reflects subtle contributions from the presence of the central ion, and has no direct bearing on the relevance of the vacancy model. The deduced signs of the individual orbital stress coefficients were found to be the same for both,[11] as required.)

Anderson, Ham, and Watkins[11] introduced spin-orbit interaction, treating it on equal footing with respect to the trigonal distortion and in second order with respect to the tetragonal distortion. The major effect was a competition between the trigonal distortion and the spin-orbit interaction for the makeup of the states derived from the $e$ orbitals [see Fig. 2(d)], which in turn strongly affected the EPR parameters of the defect as determined by the partially occupied state. The smaller second-order admixture of the excited $a_1$ state into the partially occupied EPR active state was less important and its admixture coefficient was estimated to be only $\sim 0.1$ from its effect on the $g$ values and the central hyperfine interaction.

In what follows, we follow therefore the treatment by Anderson, Ham, and Watkins,[11] but we will ignore the small spin-orbit-induced admixture of the excited $a_1$ state, which will be sufficient to illustrate the general features of the model. We expect this to be increasingly valid as we go from $Pt_s^-$ to $Pd_s^-$ to $Ni_s^-$ because of the decreasing atomic spin-orbit interaction $\zeta_d$ (3368 to 1416 to 603 $cm^{-1}$).[17]

Introducing a linear Jahn-Teller coupling constant $V$, and the elastic restoring force constant $k$ for the trigonal $t_{2z}$ distortion coordinate $Q$, plus a spin-orbit interaction $\lambda \mathcal{L} \cdot \mathbf{S}$, the orbital $e$ state with spin reduces to a simple 2×2 Hamiltonian for each spin state,

$$\mathcal{H} = \begin{vmatrix} -VQ & \pm i\frac{\lambda}{2} \\ \mp i\frac{\lambda}{2} & +VQ \end{vmatrix} + \frac{1}{2}kQ^2, \tag{1}$$

where the upper and lower signs of the off-diagonal elements go with the $M = +\frac{1}{2}$ and $-\frac{1}{2}$ states, respectively. Here, and in what follows, we use the usual convention of treating the $t_2$ manifold as an effective $\mathcal{L} = 1$ system with the corresponding matrix elements of $p$ functions. The sign of $\lambda$ is therefore reversed (negative) from that appropriate for $d$-function matrix elements, and reduced from the atomic value by $\lambda \approx -\zeta_d N^2$, where $N^2$ is the percentage central ion $d$ function in the $e$ orbitals. The

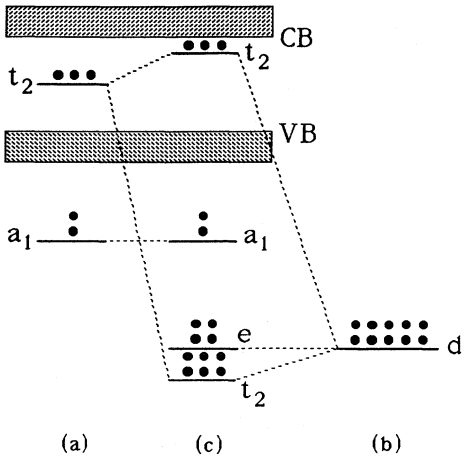


FIG. 1. One-electron energy levels of (a) the negative silicon vacancy in full tetrahedral symmetry, (b) the $d^{10}$ states of the transition-element impurity, and (c) the substitutional impurity in silicon (with no JT distortion).

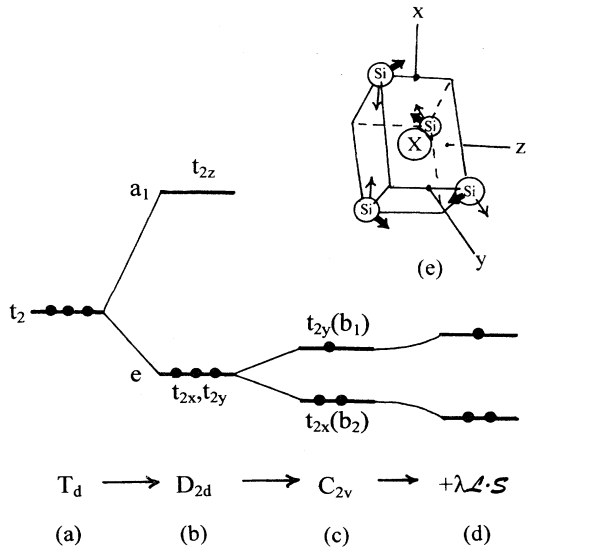


FIG. 2. Gap $t_2$ states for $Ni_s^-$, $Pd_s^-$, $Pt_s^-$, or $Au_s^0$ (a) in $T_d$ symmetry, (b) after tetragonal JT distortion, (c) plus trigonal $t_{2z}$ JT distortion, and (d) plus spin-orbit interaction. In (e), the tetragonal distortion is indicated by heavy arrows, the $t_{2z}$ trigonal distortion, by light arrows.

solution can be written compactly as

$$E/(E_{JT})_0 = \pm\frac{1}{2}\sqrt{\alpha^2+16x^2}+x^2, \tag{2}$$

where $\alpha = \lambda/(E_{JT})_0$, and $x = Q/Q_0$, with $(E_{JT})_0 = V^2/2k$ , the minimum energy at $Q_0 = V/k$, when $\lambda = 0$. The results, shown in Fig. 3 for various values of $\alpha$, illustrate the competition between $\lambda$ and the Jahn-Teller effect. The magnitude of the distortion, given by the minimum energy position $x_m$, is given by

$$x_m = \sqrt{1-(\alpha/4)^2}, \tag{3}$$

which decreases with increasing $|\lambda|$, becoming zero when $|\lambda| \geq 4(E_{JT})_0$.

Introducing the Zeeman Hamiltonian and including the hyperfine interaction of the central ion,

$$\mathcal{H}_Z = g_e\mu_B\mathbf{B}\cdot\mathbf{S}+g_{\mathcal{L}}\mu_B\mathbf{B}\cdot\mathcal{L}+g_eg_n\mu_B\mu_N\mathbf{I}\cdot\left[\frac{\mathbf{L}}{r^3}-\frac{\mathbf{S}}{r^3}+3\frac{\mathbf{r}\cdot(\mathbf{S}\cdot\mathbf{r})}{r^5}+\frac{8}{3}\pi\mathbf{S}\delta(r)\right], \tag{4}$$

an effective spin Hamiltonian for the upper (half-filled, paramagnetic) state can be written

$$\mathcal{H} = \mu_B\mathbf{B}\cdot\mathbf{g}\cdot\mathcal{S}+\mathcal{S}\cdot\mathbf{A}\cdot\mathbf{I}, \tag{5}$$

where

$$g_{zz} = g_e - 2g_{\mathcal{L}}\sqrt{1-x_m^2} = g_e + 2N^2\sqrt{1-x_m^2},$$

$$g_{xx} = g_{yy} = g_\perp = g_e x_m,$$

$$A_{xx} = A_c x_m + \frac{2}{7}PN^2\left[1+\frac{1}{2}(1-x_m)-\frac{3}{2}\sqrt{1-x_m^2}\right],$$

$$A_{yy} = A_c x_m - \frac{4}{7}PN^2\left[1-\frac{1}{4}(1-x_m)-\frac{3}{4}\sqrt{1-x_m^2}\right],$$

$$A_{zz} = A_c + \frac{2}{7}PN^2\left[1+7\sqrt{1-x_m^2}\right]. \tag{6}$$

Here, $A_c$ is the Fermi contact term, $P = g_eg_N\mu_B\mu_N\langle r^{-3}\rangle_{av}$ for the $5d$, $4d$, or $3d$ orbital on the central ion, $N^2$ is the percentage $d$ character in the orbital, and $\mathcal{S}$ is an effective $\mathcal{S} = 1/2$ spin operator.

In the case of $Pt_s^-$, the near axial symmetry for the $g$ tensor, with $g_{xx} \approx g_{yy} \approx 1.4$ (see Table I), gives $x_m \approx 0.7$, which, with Eq. (3), indicates $\alpha = \lambda/(E_{JT})_0 \approx 2.8$. For it, therefore, the competition between spin orbit and the trigonal distortion is a very close one, which is evident also in Fig. 3 for $x_m = 0.7$ , where the distortion is just barely able to occur. With these values, a reasonable match to the $^{195}Pt$ hyperfine-tensor values could be made with $A_c = -227\times10^{-4}$ cm$^{-1}$ and $PN^2 = 59\times10^{-4}$ cm$^{-1}$. With $P = 425\times10^{-4}$ cm$^{-1}$ for a Pt $5d$ orbital,[18] this gives $N^2 = 0.14$ for the fraction $5d$ character in the orbital. An improved fit was obtained both to $g_{zz}$ and to the hyperfine values by including a small admixture of the $a_1$ state into the $t_{2y}$ orbital ($\sim$0.1), leading to $A_c = -219\times10^{-4}$ cm$^{-1}$ and $PN^2 = 49\times10^{-4}$ cm$^{-1}$, and $N^2 = 0.12$. The conclusion of these authors was therefore that the vacancy model did indeed account for

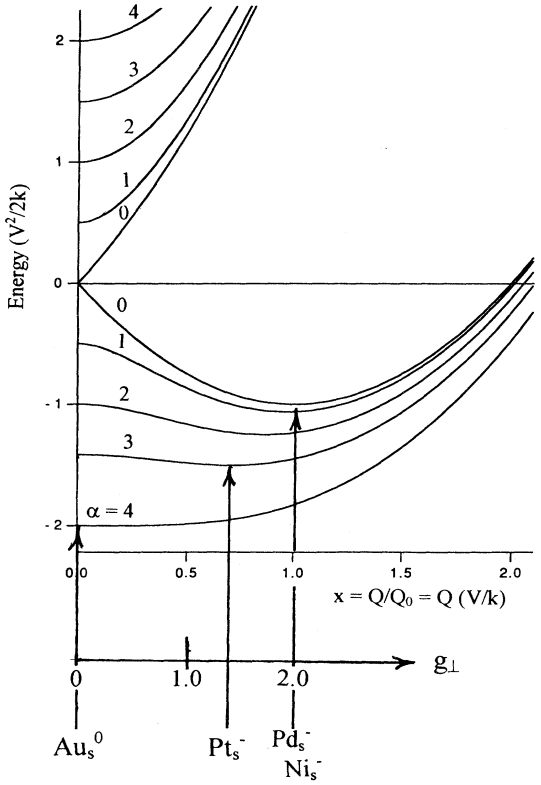


FIG. 3. Energy vs the JT trigonal distortion coordinate $Q$, for the two lowest-energy states of the defect for various values of $\alpha = \lambda/(E_{JT})_0$. The relationship between $g_\perp$ and the minimum energy position is indicated, along with the corresponding implied position for each of the impurities.

TABLE I. Spin-Hamiltonian parameters for $^{61}Ni_s^-$, $^{105}Pd_s^-$, $^{195}Pt_s^-$, and $^{197}Au_s^0$. The hyperfine components are given in MHz.

| Impurity | Tensor | $xx$ | $yy$ | $zz$ | Ref. |
|---|---|---|---|---|---|
| $^{61}Ni_s^-$ | $g$ | 2.0182 | 2.0536 | 2.0163 | 13,23 |
| | $g_N$ | 0.665 | -0.328 | 0.324 | 13 |
| | $A$ | -39.98 | -37.60 | +1.01 | 13 |
| | $A$ | **-39.98** | **+37.60** | **+1.01** | This paper |
| $^{105}Pd_s^-$ | $g$ | 1.9715 | 1.9190 | 2.0544 | 13,32 |
| | $g_N$ | -0.2515 | +0.2761 | -0.2578 | 13 |
| | $A$ | 36.01 | 35.11 | 19.28 | 13 |
| | $A$ | **-36.01** | **+35.11** | **-19.28** | This paper |
| $^{195}Pt_s^-$ | $g$ | 1.3867 | 1.4266 | 2.0789 | 32 |
| | $A$ | -440.7 | -552.2 | -380.7 | 32 |
| $^{197}Au_s^0$ | $g$ | $\sim$0 | $\sim$0 | $\sim$2.8 | 14,15 |

all of the essential features of the $Pt_s^-$ spectrum, and that the electrically active $t_2$ orbitals in the band gap contain ~10–15 % $5d$ character.

## III. SUBSTITUTIONAL $Au_s^0$ IN SILICON

Zeeman studies of both the electron and hole excitation spectra to Coulombically bound effective-mass excited states of neutral substitutional gold in silicon have been reported.[19,20] The energies of each of the transitions firmly establish the origin of the transitions as those of the dominant defect produced by gold in silicon, with an acceptor level at $E_V + 0.62$ eV and a donor level at $E_V + 0.35$ eV.[21] From these studies, the ground state of the neutral defect was determined to have $C_{2v}$ symmetry, and, like its isoelectronic analog $Pt_s^-$, could reorient easily at $T < 4$ K. This ease of reorientation established unambiguously that it is isolated, not a complex, its low symmetry the result of Jahn-Teller distortions. The sense of alignment under uniaxial stress was also established to be identical to that for $Pt_s^-$, confirming the level structure as indicated in Fig. 2. Further strong evidence that it arises from *isolated substitutional* gold comes from deep-level transient spectroscopy studies,[22] where it was demonstrated that in the radioactive decay of $^{195}$Au to $^{195}$Pt, the $E_V+0.62$ and $E_V+0.35$ eV levels convert in 1:1 fashion to an $E_C-0.22$ eV acceptor level, which has been well established to arise from isolated $Pt_s$. The Zeeman studies determined that the ground state splits according to an effective $\mathcal{S} = 1/2$, with $g_{\|} \approx 2.8$ and $g_{\perp} \approx 0$.

(Recently, a $C_{2v}$ EPR signal with small $g$ anisotropy has been reported in Ag-doped silicon and attributed to isolated substitutional $Au^0$, accidentally introduced in the processing.[23] In view of the strong evidence cited above, we suggest that this EPR signal, if related to gold at all,[20] must arise from a Au-defect complex, as has been established for all other Au-related EPR signals previously reported in silicon.[24–27] The good agreement to be shown below of the optically determined $g$ values with those predicted by the vacancy model further confirms this conclusion.)

A glance at Fig. 3 demonstrates how this also fits well into our simplified treatment of the vacancy model. In the case of $Au_s^0$, the increased atomic spin-orbit interaction $\zeta_d$ (4910 for $Au^0$ vs 3368 $cm^{-1}$ estimated from atomic splittings for $Pt^+$) (Ref. 28) and increased $N^2$, expected for its deeper acceptor state ($E_C-0.56$ eV vs $E_C - 0.22$ eV for $Pt_s$), is sufficient for $\alpha = \lambda/(E_{JT})_0 = \zeta_{Au}N^2/(E_{JT})_0 \rightarrow 4$ and $x_m \rightarrow 0$, giving $g_{\perp} = 0$. The value of $g_{zz} \approx 2.8$ is also consistent with this, implying $N^2 \approx 40\%$.

The fact that one has $g_{\perp} = 0$ is sufficient to explain the failure to observe isolated $Au_s^0$ by EPR, because of the vanishing microwave transition probability between the states.[29,11] Random strains can, of course, produce small departures from this condition, and in a few similar $g_{\perp} = 0$ cases (other ions, other lattices),[30,31] EPR has been observed, though weakly. However, in the case of $Au_s^0$, the shallow potential well implied in Fig. 3 undoubtedly adds further dynamic complications, which could serve to severely broaden the weak transitions.

## IV. EPR RESULTS FOR $Pd_s^-$ AND $Ni_s^-$ IN SILICON

EPR studies have revealed that $Pd_s^-$ and $Ni_s^-$ also have $C_{2v}$ symmetry.[12,13,32,33] Under uniaxial stress, the defects have been shown to behave in a manner identical to $Pt_s^-$ and $Au_s^0$, both in the ease with which they can reorient (at $T \leq 4.2$ K) and in the sense of alignment.[34] The signs of both the tetragonal and trigonal distortions are therefore identical to those of $Pt_s^-$ and $Au_s^0$, consistent with the level structure indicated in Fig. 2.

The results of recent analysis of the spin-Hamiltonian parameters for $Pd_s^-$ using EPR and ENDOR,[12,13] and for $Ni_s^-$ using EPR,[13,33] are given in Table I. For each, resolved hyperfine interactions are observed for only two of the four silicon neighbors. The axis labeling in the table has been chosen so that each conforms to Fig. 1, with the two Si atoms in the $xz$ plane. In the analysis, it was necessary to expand the Hamiltonian of Eq. (5) to include quadrupole interactions for the $I = 5/2$ $^{105}$Pd and $I = 3/2$ $^{61}$Ni nuclei, $\mathbf{I} \cdot \mathbf{Q} \cdot \mathbf{I}$, and their direct interaction with the external field, $-\mu_N \mathbf{I} \cdot \mathbf{g}_N \cdot \mathbf{B}$.

For these ions, the vacancy model predicts $x_m \rightarrow 1$ as we go from $Pt_s^-$ to $Pd_s^-$ to $Ni_s^-$, because of the progressive decrease in the free atom spin-orbit interaction (3368 to 1416 to 603 $cm^{-1}$).[17] This trend is clear from the value of $(g_{xx} + g_{yy})/2$ which goes from 1.407 to 1.945 to 2.036, and from the value of $g_{zz}$ which goes from 2.0789 to 2.0544 to 2.0160. For $Pd_s^-$, the value of $(g_{xx} + g_{yy})/2 = 1.945$ corresponds with Eqs. (6) to $x_m \approx 0.97$, which, with $g_{zz} = 2.0544$, gives $N^2 \approx 0.11$. There are of course other contributions to the $g$ shifts (spin-orbit interactions at the Si neighbors, etc.), which become relatively more important as we progress toward Ni, and it is clear that the simple formulas can no longer be used in this fashion for $Ni_s^-$, where $(g_{xx} + g_{yy})/2 > 2.0023$. We can conclude, however, that $x_m \approx 1$, as further evidenced by the value of $g_{zz}$. The $g$ values for all three ions, therefore, also fit satisfactorily into the vacancy model, and the relevance of this for the spin-orbit vs Jahn-Teller competition in the $e$ state is indicated in Fig. 3.

However, the hyperfine interaction with the central ion should, according to Eqs. (6), approach axial symmetry around the $y$ axis and instead it is given as almost axially symmetric around the $z$ axis in Table I. It is this observation that led the authors of these two papers[12,13] to conclude that the vacancy model was not applicable for these impurities.

In the results for $Pd_s^-$, the ENDOR transitions for $M = +1/2$ and $M = -1/2$ were found to cross as $\mathbf{B}$ was rotated in certain of the defect planes. To explain this, the authors concluded that the nuclear $\mathbf{g}_N$-tensor components must change sign in these planes, as indicated in the table, and a good fit to the ENDOR and EPR spectra was then achieved. A similar analysis was therefore made for the $Ni_s^-$ EPR spectrum, as indicated also in the table. They suggested that such an effect could result from orbital angular momentum mixed into the wave function and argued that this large anisotropy of the nuclear $g$ tensor represented an additional argument

against the vacancy model because it is not observed in the ENDOR of $V^-$. (For $Pd_s^-$, there is an ambiguity as to which particular planes have this property. In the first paper,[12] it is the $xz$ and $xy$ planes. In the later paper by this group,[13] it is the $yz$ and $yx$ planes. The results shown in Table I have been taken from the later reference.[13])

We argue that such a large anisotropy for $\mathbf{g}_N$ is not physically reasonable. As pointed out by Ludwig and Woodbury,[35] orbital angular momentum can indeed introduce anisotropy into the nuclear $g$ value, as it does into the electronic $g$ value, but the two contributions are related,

$$\Delta g_N = \Delta g P N^2 \mu_B / \lambda \mu_N. \tag{7}$$

From this relationship, an anisotropy of $\leq 1\%$ is predicted.

An alternative analysis could have been made by changing the sign of $A_{yy}$ with respect to those of $A_{xx}$ and $A_{zz}$ and keeping the signs of the $\mathbf{g}_N$ components unchanged. That this would also produce very similar ENDOR results can be seen as follows: The nuclear Hamiltonian, accurate to first order in $A/g\mu_B B$, can be written

$$\mathcal{H}_N = -g_{N_0}\mu_N \mathbf{I}\cdot\left(\frac{\mathbf{g}_N\cdot\mathbf{B}}{g_{N_0}} - \frac{\mathbf{A}\cdot\mathbf{g}\cdot\mathbf{B}}{g_{N_0}\mu_N|\mathbf{g}\cdot\mathbf{B}|}M\right) + \mathbf{I}\cdot\mathbf{Q}\cdot\mathbf{I}, \tag{8}$$

where $g_{N_0}$ denotes the normal nuclear $g$ value. Written this way, the term in the parentheses is the magnetic field seen by the nucleus. Its magnitude and the magnitude of its components along the principal $x, y, z$ axes of the defect (i.e., of $\mathbf{g}$, $\mathbf{A}$, $\mathbf{g}_N$, and $\mathbf{Q}$) are unchanged by the interchange of signs between common components of $\mathbf{g}_N$ and $\mathbf{A}$ (only the signs of the components change), and the nuclear energy levels and transitions given by Eq. (8) are therefore *identical.* [This is confirmed by direct diagonalization of Eq. (8) for the two cases using the values in Table I. They give identical results which, in turn, match the ENDOR angular dependences given in Fig. 2 of Ref. 12 for the $m = \frac{1}{2} \leftrightarrow -\frac{1}{2}$ transition within the accuracy afforded by the figure. For example, the crossover of the transitions will occur close to where the magnitude of the field is the same for the $M = +\frac{1}{2}$ and $-\frac{1}{2}$ states. This occurs when its two components are perpendicular to each other, i.e., $\mathbf{B}\cdot\mathbf{g}_N\cdot\mathbf{A}\cdot\mathbf{g}\cdot\mathbf{B} = 0$. In the $yz$ plane, this occurs when $(g_N)_{yy}A_{yy}g_{yy}\sin^2\theta = -(g_N)_{zz}A_{zz}g_{zz}\cos^2\theta$, where $\theta$ is the angle between $\mathbf{B}$ and the $z$ axis. This can be satisfied for the same value of $\theta$ by reversing the signs for the two components of either $\mathbf{A}$ or $\mathbf{g}_N$, which for the values given in Table I gives $\theta = 36°$, close to the value ($\sim 32°$) estimated from Fig. 2 in Ref. 12 for the crossover of the ENDOR transitions in that plane. Including the quadrupole interaction shifts the crossing to 32° because the orientation of the field changes slightly even though its magnitude does not.] Second-order correction terms can produce shifts in the transitions of $A^2/4g\mu_B B \sim 14$ kHz, and pseudoquadrupole terms of order $A^2/6g\mu_B B \sim 10$ kHz, which in a careful analysis could potentially distinguish between the two alternative interpretations but are within the stated ±20 kHz fit of Ref. 12 for the $m = +\frac{1}{2} \longleftrightarrow -\frac{1}{2}$ transition.

We suggest therefore that the correct analysis of the EPR and ENDOR results for $Pd_s^-$, and therefore also for $Ni_s^-$, should have $A_{yy}$ of reversed sign and $g_N$ essentially isotropic, as expected, with its normal nuclear value ($-0.500$ for $^{61}$Ni and $-0.256$ for $^{105}$Pd). (Note that the values for $g_N$ in the table for $^{105}$Pd are very close to its normal nuclear value, except for sign, while those for $^{61}$Ni depart significantly. This is as expected, the values for the former coming from accurate ENDOR studies, those of the latter from a fit to the EPR results which are less sensitive to the nuclear $g$ values.) In what follows, therefore, we will use the magnitude of the hyperfine tensor components measured by these workers but with the alternative signs given by the bold values in Table I. (The absolute signs have not been determined experimentally. The signs in the table have been selected so that the anisotropic component corresponds to that predicted for the $b_1$ orbital of Fig. 2, as will be justified in the next paragraph.)

With this alternative analysis, there is now a large central ion hyperfine anisotropy in the $xy$ plane, consistent with the unpaired spin in the $b_1$ orbital, as predicted by the vacancy model, and depicted in Fig. 2. For $Ni_s^-$, with $x_m = 1$ and $P = -333 \times 10^{-4}$ cm$^{-1}$,[18] the value of $A_{yy} - (A_{xx} + A_{zz})/2 = +57.1$ MHz corresponds to $N^2 = 0.20$, a reasonable value. For $Pd_s^-$, however, the corresponding hyperfine anisotropy value of +62.7 MHz, with $x_m = 0.97$ and $P = -159$ MHz,[18] gives $N^2 = 0.46$. This is substantially larger than the estimate of 0.11 from the $g$ values and serves as warning that additional contributions to the hyperfine interaction not considered above, such as polarization of the bonding $d$ states in the valence band and of the inner $d$ and $p$ shells, contribution from admixtures of $5p$ valence states, etc., may be playing an important role. Further evidence is the departure from axial symmetry for both $Ni_s^-$ and $Pd_s^-$, i.e., $A_{xx} \neq A_{zz}$. The important point at this stage is only that *the anisotropy of the hyperfine interaction is fully consistent with $b_1$ symmetry for the partially occupied orbital, as predicted from the vacancy model.* A fully quantitative agreement for the hyperfine interaction may require a more sophisticated treatment including the various exchange polarization effects.

## V. SUMMARY

The vacancy model[1] predicts that the electronic structure of substitutional $3d$, $4d$, and $5d$ transition-element impurities near the end of each series in silicon can be understood as having filled $d$ shells, deep in the valence band, with the remaining electrons in $t_2$ gap orbitals which are primarily those of the "vacancy" into which they are inserted. Only modest admixtures of the $t_2$ impurity $d$ orbitals are expected. An alternative analysis of published EPR (Refs. 13 and 33) and ENDOR (Refs. 12 and 13) results for $Ni_s^-$ and $Pd_s^-$ has been proposed, which we argue is physically more reasonable. With this, $Ni_s^-$, $Pd_s^-$, $Pt_s^-$, and $Au_s^0$ now all fit well

into the general predictions of the model, as described in a simplified treatment we have presented of the theory of Anderson, Ham, and Watkins.[11] This treatment contains the essential physics of the system—the competition between spin-orbit interaction and an off-center Jahn-Teller displacement of the substitutional ion—and provides a simple graphical display (Fig. 3) for the $g$ values and the magnitude of the distortion vs the relative size of the spin-orbit and Jahn-Teller interactions. Detailed quantitative agreement with the central hyperfine interactions is not achieved, particularly for $Pd_s^-$, but it is argued that exchange polarization effects, not included in the treatment, are probably responsible.

Finally, we point out that it would be highly desirable that the ENDOR for $Pd^-$ be repeated (unfortunately, the original data are no longer available for reanalysis[36]) and carefully analyzed to establish whether $\mathbf{g}_N$ changes sign as suggested in Ref. 12, or behaves as normally expected, as we have proposed here.

## ACKNOWLEDGMENTS

Helpful discussions with Frank Ham are gratefully acknowledged. The research was supported by the U.S. Navy Office of Naval Research (Electronics and Solid State Sciences Program) under Grant No. N00014-90-J-1264.

[1] G. D. Watkins, Physica B+C **117B-118B**, 9 (1983).
[2] L.A. Hemstreet, Phys. Rev. B **15**, 834 (1976).
[3] A. Zunger and U. Lindefelt, Phys. Rev. B **27**, 1191 (1983).
[4] J. L. A. Alves and J. R. Leite, Phys. Rev. B **30**, 284 (1984).
[5] F. Beeler, O. K. Andersen, and M. Scheffler, Phys. Rev. Lett. **55**, 1598 (1985).
[6] C. Delerue, M. Lannoo, and G. Allan, Phys. Rev. B **39**, 1669 (1989).
[7] C. A. J. Ammerlaan and A. B. van Oosten, Phys. Scr. **T25**, 342 (1989).
[8] C. Delarue, F. G. Anderson, and M. Lannoo, in *The Physics of Semiconductors*, edited by E. M. Anastassakis and J. D. Joannopoulos (World Scientific, Singapore, 1990), p. 585.
[9] F. G. Anderson, C. Delarue, M. Lannoo, and G. Allan, Phys. Rev. B **44**, 10 925 (1991).
[10] J. E. Lowther, J. Phys. C **13**, 3681 (1980).
[11] F. G. Anderson, F. S. Ham, and G. D. Watkins, Phys. Rev. B **45**, 3287 (1992).
[12] A. B. van Oosten, N. T. Son, L. S. Vlasenko, and C. A. J. Ammerlaan, Mater. Sci. Forum **38-41**, 355 (1989).
[13] N. T. Son, A. B. van Oosten, and C. A. J. Ammerlaan, Solid State Commun. **80**, 439 (1991).
[14] G. D. Watkins, *Effets des Rayonnements sur les Semiconducteurs* (Academic Press, New York, 1964), p. 97.
[15] F. G. Anderson, R. F. Milligan, and G. D. Watkins, Phys. Rev. B **45**, 3279 (1992).
[16] M. Lannoo, Phys. Rev. B **36**, 9355 (1987).
[17] The ground-state ($5d^9\ ^2D$) spin-orbit splitting of the free-ion positive-charge state is approximated by $-(5/2)\zeta_d$ [C. E. Moore, *Atomic Energy Levels*, Natl. Bur. Stand. (U.S.) Circ. No. 467 (U.S. GPO, Washington, D.C., 1958)].
[18] A. K. Koh and D. J. Miller, At. Data Nucl. Data Tables **33**, 235 (1985).
[19] G. D. Watkins, M. Kleverman, A. Thilderkvist, and H. G. Grimmeiss, Phys. Rev. Lett. **67**, 1149 (1991).
[20] M. Kleverman, A. Thilderkvist, G. Grossmann, H. G. Grimmeiss, and G. D. Watkins, Solid State Commun. **93**, 383 (1995).
[21] C. B. Collins, R. O. Carlson, and C. J. Gallagher, Phys. Rev. **105**, 1168 (1947).
[22] J. W. Petersen and J. Nielsen, Appl. Phys. Lett. **56**, 1122 (1990).
[23] N. T. Son, T. Gregorkiewicz, and C. A. J. Ammerlaan, Phys. Rev. Lett. **69**, 3185 (1992).
[24] G. W. Ludwig and H. H. Woodbury, in *Solid State Physics*, edited by F. Seitz and D. Turnbull (Academic Press, New York, 1962), p. 223.
[25] M. Höhne, Phys. Status Solidi B **99**, 651 (1980); **109**, 525 (1982); **119**, K117 (1983); **138**, 337 (1986).
[26] R. L. Kleinhenz, Y. H. Lee, J. W. Corbett, E. G. Sieverts, S. H. Müller, and C. A. J. Ammerlaan, Phys. Status Solidi B **108**, 363 (1981).
[27] E. G. Sieverts, S. H. Müller, C. A. J. Ammerlaan, R. L. Kleinhenz, and J. W. Corbett, Phys. Status Solidi B **109**, 83 (1982).
[28] The ground-state ($5d^9 6s^2\ ^2D$) spin-orbit splitting of the Au free-ion neutral-charge state is approximated by $-(5/2)\zeta_d$ [C. E. Moore, *Atomic Energy Levels* (Ref. 17)].
[29] F. G. Anderson, Bull. Am. Phys. Soc. **36**, 862 (1991).
[30] K. Maier, H. D. Müller, and J. Schneider, Mater. Sci. Forum **83-86**, 1183 (1992).
[31] J. Isoya, H. Kanda, and Y. Uchida, Phys. Rev. B **42**, 9843 (1990).
[32] H. H. Woodbury and G. W. Ludwig, Phys. Rev. **126**, 466 (1962).
[33] L. S. Vlasenko, N. T. Son, A. B. van Oosten, C. A. J. Ammerlaan, A. A. Lebedev, E. S. Taptygov, and V. A. Khramtsov, Solid State Commun. **73**, 393 (1990).
[34] P. M. Williams, F. S. Ham, F. G. Anderson, and G. D. Watkins, Mater. Sci. Forum **83-87**, 233 (1992).
[35] G. W. Ludwig and H. H. Woodbury, Phys. Rev. **117**, 1286 (1960).
[36] C. A. J. Ammerlaan (private communication).